JOURNAL OF PROPULSION AND POWER
Vol. 11, No. 2, March–April 1995

Blade Row Interaction Effects on Flutter and Forced Response

Daniel H. Buffum*
NASA Lewis Research Center, Cleveland, Ohio 44135

A procedure to calculate intrablade row unsteady aerodynamic interactions is developed that relies upon results from isolated blade row unsteady aerodynamic analyses. Using influence coefficients that express the unsteady forces on one blade row due to the motion of another, an aeroelastic model is obtained that accounts for the coupling of the vibratory responses of multiple blade rows. The model is applied to two model configurations, each consisting of three blade rows. The flutter analysis shows that interaction effects can be destabilizing, and the forced response analysis shows that interaction effects can result in a significant increase in the resonant response of a blade row.

Introduction

IN the flutter analysis of a turbomachine blade row, the blade row is commonly assumed to be isolated—disturbances created by the vibrating blades are free to propagate away from the blade row without being disturbed. Therefore, any reflections of these outgoing waves by other structural members or nonuniformities in the mean-flowfield are neglected. Although the forced response problem is typically concerned with blade row interaction, forced response analyses also generally neglect any reflections of outgoing waves. However, in an engine environment, structural elements such as neighboring blade rows or struts and nonuniformities in the mean-flowfield will reflect some of this wave energy back toward the vibrating blades, causing additional unsteady forces on them. Whether or not these reflected waves can significantly affect the aeroelastic stability or forced response of a blade row is a question of fundamental importance.

Several investigations have focused on the unsteady aerodynamic interaction between two rigid blade rows. Kaji and Okazaki[1] investigated the interaction of two blade rows for the purpose of predicting rotor-stator interaction noise. They obtained a simultaneous solution to the unsteady lift distributions on both of the blade rows. Hanson[2] modified Smith's[3] isolated blade row unsteady aerodynamic analysis to predict rotor-stator interaction noise, essentially extending Kaji and Okazaki's work to include effects of frequency scattering and mean-flow turning by the blade rows. For a counter-rotating propfan in incompressible flow, Chen and Williams[4] used a panel method to determine the unsteady loads on rigid propeller blades. From the point-of-view of the present investigation, all of these investigations are somewhat limited because they did not delve into the aeroelastic problem and they were limited to two blade rows.

One investigation that did consider the aeroelastic effects of interactions of a vibrating blade row and an adjacent structure was that of Williams et al.[5] A three-dimensional linearized compressible panel method was used to calculate the unsteady aerodynamics of a ducted fan. The aeroelastic analysis allowed flexibility of both the fan and the duct. The duct was found to have a destabilizing effect on the fan.

A number of time-accurate solutions to the Euler and Navier-Stokes equations for rotor-stator interaction have been presented.[6–8] Due to the large computing time required to obtain solutions for just two blade rows, time-marching codes such as these are not practical for routine aeroelastic analysis purposes.

The purpose of this article is to investigate the effects of blade row interaction on flutter and forced response. A model for interaction between any number of blade rows is proposed that relies upon unsteady aerodynamic coefficients obtained from isolated blade row unsteady aerodynamic analyses. This allows the use of computationally efficient linearized isolated blade row analyses, which are currently favored for turbomachinery aeroelastic predictions, for the analysis of multiple blade row unsteady aerodynamic interactions.

The linearized analyses are generally capable of providing solutions for the unsteady blade forces and the outgoing waves generated by two classes of disturbances: 1) blade motion and 2) incoming waves such as acoustic and vorticity waves. Thus, the unsteady aerodynamic coefficients that quantify the wave reflection and transmission characteristics of the (rigid) blade rows, as required to aerodynamically couple the blade rows, are provided by the linearized unsteady aerodynamic analyses. In addition, the unsteady aerodynamic coefficients due to blade motion allow the calculation of influence coefficients that express the unsteady forces on one blade row due to the motion of another. By combining the various influence coefficients with equations of motion for each of the blade rows, a system of equations may be obtained that models what will be referred to as the "dynamic coupling" of flexible blade rows.

In this article, a model for unsteady aerodynamic interaction between any number of blade rows is developed. The coupled equations of motion for the flexible blade rows, which rely upon unsteady aerodynamic influence coefficients for the intrablade row coupling, are derived. A system of linear equations is found for the unsteady aerodynamic influence coefficients. Whitehead's[9] subsonic flat-plate cascade analysis, Linsub, is used to provide the unsteady aerodynamic input for the influence coefficient solution, although this model is suitable for use with the predictions of more sophisticated isolated blade row analyses that account for nonuniform mean-flowfields.[10–12] Before applying this technique to aeroelastic problems, the predictions of the unsteady aerodynamic model are compared with those of Kaji and Okazaki[1] for outgoing acoustic wave amplitudes due to rotor-stator interaction. Then the model is used to investigate the effects of blade row interaction on the flutter and forced response of systems of three blade rows.

Analysis

Equations of Motion

A single degree-of-freedom model for torsional oscillation will be used to account for the effect of blade row interaction

Presented as Paper 93-2084 at the AIAA/SAE/ASME/ASEE 29th Joint Propulsion Conference and Exhibit, Monterey, CA, June 28–30, 1993; received Aug. 28, 1993; revision received May 18, 1994; accepted for publication May 24, 1994.

*Aerospace Engineer, Turbomachinery Technology Branch, Propulsion Systems Division, M/S 77-6.

on the vibratory response of a row of identical blades. From Chiang,[13] the equation of motion for the small amplitude torsional oscillation of a two-dimensional section of a reference blade may be expressed as

$$I\frac{d^2\bar{\alpha}}{dt^2} + (1 + 2ig)I\omega_n^2\bar{\alpha} = \bar{M} \tag{1}$$

$\bar{\alpha}(t)$ is the angle of oscillation, I is the mass moment of inertia about the elastic axis, g is the structural damping coefficient, and ω_n is the undamped natural frequency. $\bar{M}$ is the unsteady aerodynamic moment per unit span about the elastic axis.

Simple harmonic motion at frequency ω and a fixed interblade phase angle is assumed. Let the oscillation angle for the reference blade be $\bar{\alpha}(t) = \alpha e^{i\omega t}$, and the unsteady aerodynamic moment be $\bar{M}(t) = Me^{i\omega t}$. Substituting these into Eq. (1) and differentiating gives

$$[-I\omega^2 + (1 + 2ig)I\omega_n^2]\alpha = M \tag{2}$$

For the purpose of calculating $\bar{M}$, the unsteady aerodynamic disturbances are assumed to be small relative to an inviscid, subsonic mean-flow, resulting in a linear problem for the first-order unsteady disturbance field. In this investigation, the unsteady disturbances are limited to acoustic and vorticity waves. Because the unsteady disturbance field is linear, the unsteady aerodynamic moment $\bar{M}$ may be determined by the superposition of motion-dependent and motion-independent parts. Typically, these moments are calculated under the assumption that the blade row under scrutiny is isolated from the other blade rows. Consider, e.g., the response of a stator embedded in a multistage turbomachine to the wakes of an upstream rotor. As a result of the unsteady interaction of the wakes with the stator, waves are created that propagate away from the stator: acoustic waves propagate both upstream and downstream, and vorticity waves convect downstream. If the stator is treated as an isolated blade row, these waves are free to propagate away from the stator undisturbed. In reality, these waves will impact neighboring blade rows (Fig. 1). Even if the neighboring blade rows are perfectly rigid, they will emit additional acoustic and vorticity waves in response to the waves from the stator, and these waves, in turn, may further load the stator, which then emits more waves in response, etc. Through these waves the blade rows are aerodynamically coupled.

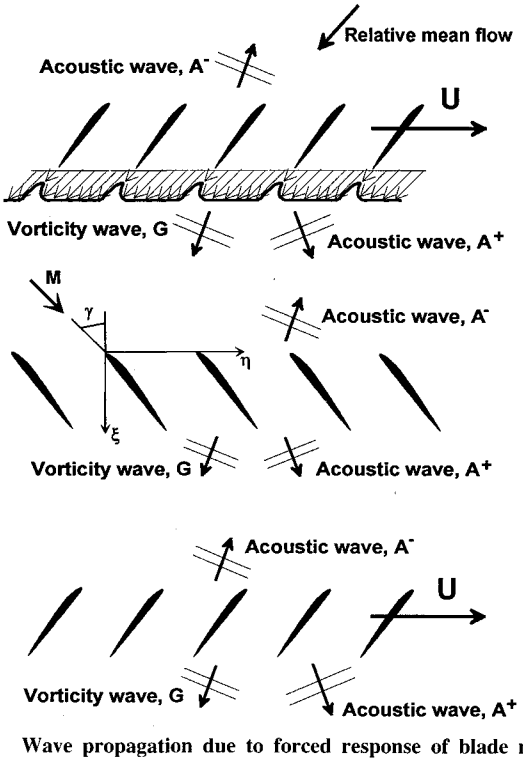

Fig. 1 Wave propagation due to forced response of blade row in multistage turbomachine.

One may carry this a step further and consider the vibratory response of the neighboring blade rows to the waves initiated by the stator/wake interaction. By allowing all of the blades to be flexible, they will respond by vibrating and emitting additional vibration-dependent waves. These motion-generated waves will further load the stator and result in additional waves ad infinitum. By allowing all of the blade rows to be flexible, they become dynamically coupled.

Since the unsteady aerodynamic problem is assumed to be linear, superposition can be used to express the aerodynamic blade row interactions as nondimensional aerodynamic influence coefficients. Let C_{jk} be the complex-valued nondimensional moment coefficient for blade row j due to oscillation of blade row k, which includes effects due to wave interaction (i.e., reflection and transmission of acoustic waves, shed vorticity) with the other nonvibrating blade rows. Thus, C_{jj} is the moment coefficient on blade row j due to its own oscillations. These influence coefficients can be used to dynamically couple any number of blade rows. For a system of n blade rows, Eq. (2) will be applied to each row, and the unsteady aerodynamic influence coefficients will be used to express the moment in Eq. (2) as the linear combination of the influences of all of the blade rows. Consider the forced response of blade row j due to a wake from an upstream blade row. It is assumed that the wake has been decomposed into spatial harmonics, and a single harmonic will be analyzed that excites row j at frequency ω_j. The unsteady aerodynamic moment on a reference blade of that row is

$$\bar{M}_j = \rho_j V_j^2 c_j^2 \left[C_{j1}\alpha_1 + C_{j2}\alpha_2 + \cdots + C_{jj}\alpha_j + \cdots + C_{jn}\alpha_n + (CG)_{j1}\frac{w_1}{V_1} + (CG)_{j2}\frac{w_2}{V_2} + \cdots + (CG)_{jj}\frac{w_j}{V_j} + \cdots + (CG)_{jn}\frac{w_n}{V_n} \right] \tag{3}$$

ρ_j is the gas density, V_j is the relative inlet velocity, and c_j is the chord length of row j. α_k is the complex-valued angle of oscillation of the reference blade of row k. $(CG)_{jk}$ is the nondimensional, complex-valued moment coefficient for row j due to a gust acting on a rigid row k with upwash w_k—typically $(CG)_{jk}$ is used to model the effects of viscous wakes. To simplify the notation, Eq. (3) was obtained with the assumption that each blade row k oscillates at only one frequency ω_k, which excites row j at frequency ω_j. If this is not the case, then an additional motion-dependent term must be added to Eq. (3) for each additional frequency.

Substituting Eq. (3) into Eq. (2), then rearranging into a nondimensional form results in

$$C_{j1}\alpha_1 + C_{j2}\alpha_2 + \cdots + \left\{ \frac{\pi}{16}\bar{\omega}_j^2 r_j^2 \mu_j \left[1 - (1 + 2ig_j)\frac{\omega_{nj}^2}{\omega_j^2} \right] + C_{jj} \right\} \alpha_j + \cdots + C_{j(n-1)}\alpha_{n-1} + C_{jn}\alpha_n = -\sum_{k=1}^{n} \frac{w_k}{V_k}(CG)_{jk} \tag{4}$$

$i = \sqrt{-1}$, $\bar{\omega}_j = (\omega_j c/V_j)$ is the reduced frequency, $r_j = \sqrt{[I_j/m_j(c_j/2)^2]}$ is the nondimensional radius of gyration of the blade section, and $\mu_j = [m_j/\pi\rho(c_j/2)^2]$ is the mass ratio of that

section. Letting $S_j = (\pi/16)\bar{\omega}_j^2 r_j^2 \mu_j[1 - (1 + 2ig_j)\gamma_j]$, where $\gamma_j = \omega_{uj}^2/\omega_j$, Eq. (4) becomes

$$C_{j1}\alpha_1 + \cdots + (S_j + C_{jj})\alpha_j + \cdots + C_{jn}\alpha_n = -\sum_{k=1}^{n} \frac{w_k}{V_k}(CG)_{jk} \tag{5}$$

A more general form of Eq. (5) may be obtained that applies to any blade row l:

$$\sum_{k=1}^{n} (s_{lk} + C_{lk})\alpha_k = -\sum_{k=1}^{n} \frac{w_k}{V_k}(CG)_{lk} \tag{6}$$

where $s_{lk} = S_l$ when $k = l$, but is otherwise zero.

Applying Eq. (6) to each of the n blade rows, a linear system of equations is obtained that may be solved for the dynamics of these blade rows due to a gust acting on row j. This system may be expressed as

$$Ax = B \tag{7}$$

where

$$A = \begin{bmatrix} S_1 + C_{11} & C_{12} & \cdots & C_{1(n-1)} & C_{1n} \\ C_{21} & S_2 + C_{22} & \cdots & C_{2(n-1)} & C_{2n} \\ \vdots & \vdots & \ddots & \vdots & \vdots \\ C_{(n-1)1} & C_{(n-1)2} & \cdots & S_{n-1} + C_{(n-1)(n-1)} & C_{(n-1)n} \\ C_{n1} & C_{n2} & \cdots & C_{n(n-1)} & S_n + C_{nn} \end{bmatrix} \tag{8a}$$

$$x = (\alpha_1, \alpha_2, \ldots, \alpha_{n-1}, \alpha_n)^T \tag{8b}$$

$$B = \left(\sum\nolimits_1', \sum\nolimits_2', \ldots, \sum\nolimits_{n-1}', \sum\nolimits_n'\right)^T \tag{8c}$$

where

$$\sum\nolimits_l' = -\sum_{k=1}^{n} \frac{w_k}{V_k}(CG)_{lk}$$

Specifying $B = 0$ in Eq. (7) results in a homogeneous system appropriate for evaluation of the system stability:

$$Ax = 0 \tag{9}$$

A meaningful solution exists only if the determinant of the coefficient matrix A is equal to zero.

For any blade row l, the structural coefficients r_l, μ_l, and g_l are assumed to be known. To investigate the stability of a particular blade row j, the real part of the reduced frequency for that row, $\mathrm{Re}(\bar{\omega}_j)$, is chosen. As shown by Buffum,[14] ω_l is related to ω_j through the relation

$$\omega_l = \omega_j + m(U_l - U_j) \tag{10}$$

m is the real-valued tangential wave number of a disturbance, and the U are the real-valued tangential speeds of the blade rows. The frequencies will generally be complex, so that from Eq. (10), $\mathrm{Re}(\omega_l) = \mathrm{Re}(\omega_j) + m(U_l - U_j)$ and $\mathrm{Im}(\omega_l) = \mathrm{Im}(\omega_j)$. The real part of Eq. (10) is used to relate the real part of the reduced frequency of row l to that of row j:

$$\mathrm{Re}(\bar{\omega}_l) = \mathrm{Re}(\bar{\omega}_j)\frac{V_j}{V_l}\frac{c_l}{c_j} + mc_l\left(\frac{U_l}{V_l} - \frac{U_j}{V_l}\right) \tag{11}$$

Thus, $\mathrm{Re}(\bar{\omega}_l)$, which is required input for the unsteady aerodynamic calculations, may be determined from Eq. (11) using the assumed value of $\mathrm{Re}(\bar{\omega}_j)$, velocity ratios that are assumed to be known, blade chord lengths, and the known tangential wave number. However, the frequency ratios γ_l in matrix A are unknown. To find a solution to Eq. (9), γ_l is expressed as a function of the unknown γ_j:

$$\gamma_l = \frac{\omega_{ul}^2}{\omega_{uj}^2}\frac{\omega_{uj}^2}{\omega_j^2}\frac{\omega_j^2}{\omega_l^2} = \frac{\omega_{ul}^2}{\omega_{uj}^2}\gamma_j\frac{\omega_j^2}{\omega_l^2} \tag{12}$$

In Eq. (12), the undamped natural frequencies ω_{ul} and ω_{uj} are assumed to be known, but since the ratios ω_j/ω_l are unknown, an iterative solution procedure is used to solve $\mathrm{Det}(A) = 0$. Assumed values of ω_j/ω_l are substituted into Eq. (12), then $\mathrm{Det}(A) = 0$ is solved for γ_j. Based on this value of γ_j, Eq. (10) is used to update ω_j/ω_j in Eq. (12), then $\mathrm{Det}(A) = 0$ is again solved for γ_j. Iteration continues in this manner until each ω_j/ω_l has converged within a specified tolerance.

The stability of row j is determined by the value of γ_j. Since

$$(i\omega_j/\omega_{uj}) = (i/\sqrt{\gamma_j}) \tag{13}$$

and $\bar{\alpha}_j(t) = \alpha_j e^{i\omega_j t}$, $\mathrm{Re}(i/\sqrt{\gamma_j}) = -\mathrm{Im}(\omega_j)/\omega_{uj} > 0$ implies blade row instability or flutter. $\mathrm{Im}(i/\sqrt{\gamma_j})$ is the ratio of the blade row j oscillation frequency to its natural frequency. Since $\mathrm{Im}(\omega_l) = \mathrm{Im}(\omega_j)$, instability of row j implies growing oscillations for the other blade rows in the system as well.

Coupled Blade Row Unsteady Aerodynamics

Expressions for the unsteady aerodynamic influence coefficients will now be developed. The mean-flowfield is assumed to be subsonic. Blade row geometry definitions are shown in Fig. 1.

Assume that blade row j is oscillating harmonically with unit amplitude at frequency ω_j and interblade phase angle β_j. Due to these oscillations, acoustic waves propagate both upstream and downstream, and vorticity waves are convected downstream. As shown by Buffum,[14] acoustic waves will propagate unattenuated through a uniform flowfield of Mach number $M < 1$ only if the tangential wave number m (i.e., the η component of the wave number) satisfies

$$m \lessgtr (\omega/a)(M_\eta \pm \sqrt{1 - M_\xi^2})/(1 - M^2) \tag{14}$$

M_ξ and M_η are the ξ and η components of the Mach number, respectively, ω is the frequency, and a is the speed of sound. If this condition is met, two propagating or super-resonant acoustic waves will be produced, one propagating upstream and the other downstream. The $-$ sign in Eq. (14) corresponds to the upstream-running wave, and $+$ corresponds to the downstream-running wave; the $<$ symbol corresponds to the $+$, and the $>$ corresponds to the $-$. Otherwise, the waves decay exponentially with axial distance and are said to be subresonant. To be consistent with β_j, m must satisfy

$$ms_j = \beta_j + 2\pi r, \qquad r = 0, \pm 1, \pm 2, \ldots \tag{15}$$

where s_j is the spacing of the row j blades.

As a first approximation, only super-resonant acoustic waves will be considered, even though decaying waves may be important, particularly when the gap between blade rows is small.

It would be a straightforward extension of the analysis to include decaying waves. Also, scattering of waves at the other blade rows results in waves returning to row j, which are generally not at the frequency of interest.[14] Although these waves might eventually be scattered back to the frequency of interest, they will be neglected.

Let the waves generated by the motion of row j at frequency ω_j be denoted $G_{M,j}$ for the gust or vorticity wave, $A^-_{M,j}$ for the upstream-traveling acoustic wave, and $A^+_{M,j}$ for the downstream-traveling acoustic wave. All of these are complex-valued so that both the wave amplitudes and phases are included in these coefficients. Superscript symbols $-$ and $+$ are used to indicate the directions of acoustic waves, $-$ being a wave going toward $-\infty$ (upstream), and $+$ being toward $+\infty$ (downstream). To avoid unnecessary complications in the present explanation, acoustic waves are assumed to propagate unattenuated in both the upstream and downstream directions for only one tangential wave number consistent with the interblade phase angle. Assuming that a dynamic steady state is reached for all the resulting waves, each blade row k will have the net effects of three different incoming waves acting upon it, a gust $G_{I,k}$, an upstream-running acoustic wave $A^-_{I,k}$, and a downstream-running acoustic wave $A^+_{I,k}$. The outgoing waves at row k are linearly related to the incoming waves by the various reflection and transmission coefficients of the blade row. For example, the outgoing upstream-running acoustic wave will be

$$A^-_{O,k} = A^-_{I,k}T^-_k + A^+_{I,k}R^+_k + G_{I,k}A^-_{G,k} \tag{16}$$

where, for row k, T^-_k is the transmission coefficient for the upstream-traveling acoustic wave, R^+_k is the reflection coefficient for the downstream-traveling acoustic wave, and $A^-_{G,k}$ is the upstream-running acoustic wave due to an incoming gust. Similarly, the other two outgoing waves are a linear combination of the incoming waves:

$$A^+_{O,k} = A^-_{I,k}R^-_k + A^+_{I,k}T^+_k + G_{I,k}A^+_{G,k} \tag{17}$$

$$G_{O,k} = A^-_{I,k}G^-_{A,k} + A^+_{I,k}G^+_{A,k} + G_{I,k}G_{G,k} \tag{18}$$

The new coefficients $G^-_{A,k}$, $G^+_{A,k}$, and $G_{G,k}$ are the resulting gusts or vorticity waves due to an upstream-running acoustic wave, a downstream-running acoustic wave, and a gust, respectively, incident on row k.

By defining the outgoing and incoming waves at common interfaces between the blade rows, the outgoing waves at row k are related to the incoming waves at adjacent blade rows by

$$A^-_{O,k} = A^-_{I,k-1}$$

$$A^+_{O,k} = A^+_{I,k+1}$$

$$G_{O,k} = G_{I,k+1}$$

so that Eqs. (16–18) become

$$A^-_{I,k-1} = A^-_{I,k}T_k + A^+_{I,k}R^+_k + G_{I,k}A^-_{G,k} \tag{19}$$

$$A^+_{I,k+1} = A^-_{I,k}R^-_k + A^+_{I,k}T^+_k + G_{I,k}A^+_{G,k} \tag{20}$$

$$G_{I,k+1} = A^-_{I,k}G^-_{A,k} + A^+_{I,k}G^+_{A,k} + G_{I,k}G_G \tag{21}$$

For the blade rows neighboring the oscillating row, the incoming waves may be split into known parts due to the oscillation indicated by the subscript M, and unknown parts $\hat{A}^+$, $\hat{A}^-$, and $\hat{G}$ due to the ensuing interactions with the other blade rows:

$$A^-_{I,j-1} = \hat{A}^-_{I,j-1} + A^-_{M,j}$$

$$A^+_{I,j+1} = \hat{A}^+_{I,j+1} + A^+_{M,j}$$

$$G_{I,j+1} = \hat{G}_{I,j+1} + G_{M,j}$$

Then, for row j and its immediate neighbors, the system of equations is, with all of the unknowns collected on the right side and the known terms due to the motion of row j on the left side

$$\begin{aligned}
A^-_{M,j} &= -\hat{A}^-_{I,j-1} + A^-_{I,j}T^-_j + A^+_{I,j}R^+_j + G_{I,j}A^-_{G,j}\\
0 &= -A^+_{I,j-1} + A^-_{I,j-2}R^-_{j-2} + A^+_{I,j-2}T^+_{j-2} + G_{I,j-2}A^+_{G,j-2}\\
0 &= -G_{I,j-1} + A^-_{I,j-2}G^-_{A,j-2} + A^+_{I,j-2}G^+_{A,j-2} + G_{I,j-2}G_{G,j-2}\\
-A^+_{M,j}R^+_{j+1} &- G_{M,j}A^-_{G,j+1} = -A^-_{I,j} + A^-_{I,j+1}T^-_{j+1}\\
&+ \hat{A}^+_{I,j+1}R^+_{j+1} + \hat{G}_{I,j+1}A^-_{G,j+1}\\
-A^-_{M,j}R^-_{j-1} &= -A^+_{I,j} + \hat{A}^-_{I,j-1}R^-_{j-1} + A^+_{I,j-1}T^+_{j-1}\\
&+ G_{I,j-1}A^+_{G,j-1}\\
-A^-_{M,j}G^-_{A,j-1} &= -G_{I,j} + \hat{A}^-_{I,j-1}G^-_{A,j-1} + A^+_{I,j-1}G^+_{A,j-1}\\
&+ G_{I,j-1}G_{G,j-1}\\
0 &= -A^-_{I,j+1} + A^-_{I,j+2}T^-_{j+2} + A^+_{I,j+2}R^+_{j+2} + G_{I,j+2}A^-_{G,j+2}\\
A^+_{M,j} &= -\hat{A}^+_{I,j+1} + A^-_{I,j}R^-_j + A^+_{I,j}T^+_j + G_{I,j}A^+_{G,j}\\
G_{M,j} &= -\hat{G}_{I,j+1} + A^-_{I,j}G^-_{A,j} + A^+_{I,j}G^+_{A,j} + G_{I,j}G_{G,j}
\end{aligned} \tag{22}$$

The reflection coefficients R, the transmission coefficients T, and the gust coefficients A_G, G_A, and G_G will be calculated by the isolated blade row unsteady aerodynamic analysis, so they are treated as known values in Eq. (22).

Assuming that three blade rows will be analyzed, the present system of 9 equations has 15 unknowns because the incoming waves to rows $(j-2)$ and $(j+2)$ are required. By assuming that no waves internal to the three blade row system are reflected by these two external rows, $R^-_{j-2} = G^-_{A,j-2} = R^+_{j+2} = A^-_{G,j+2} = 0$, and that there are no waves incoming from sources external to the system, $A^+_{I,j-2} = G_{I,j-2} = A^-_{I,j+2} = 0$, the number of unknowns is reduced to 9. Thus, the system of equations may be solved for the incoming waves to each of the three blade rows. Using coefficients provided by the isolated blade row analysis that relate the moment on a blade to the incoming waves, the unsteady moment on each blade row k due to oscillation of row j—the influence coefficient C_{kj}—may then be determined. Similarly, by using the waves generated by a unit amplitude gust acting on row j as the known terms in Eq. (22), the gust coefficients $(CG)_{kj}$ may also be determined.

In this investigation, Whitehead's linearized subsonic flat-plate cascade code, Linsub,[9] will be used to supply the required aerodynamic quantities. It assumes inviscid, isentropic, subsonic flow through an isolated, infinite cascade of equally spaced flat-plate airfoils. The airfoils are at zero mean incidence so that the mean-flow is uniform, and the unsteady disturbances created by the airfoil oscillations or incoming gusts are assumed to create small unsteady disturbances to the mean-flow, resulting in a linear problem for the unsteady flow. Linsub calculates moment coefficients due to oscillation of the cascade or due to incoming acoustic or vorticity gusts, and outgoing acoustic and vorticity waves due to oscillation of the cascade or due to incoming waves. Thus, all the coefficients required by Eq. (22) can be obtained from Linsub.

Results

This model for unsteady aerodynamic blade row interaction will be applied to both the flutter and forced response of the

middle blade row in a system of three blade rows. Before investigating these aeroelastic problems, the predictions of the unsteady aerodynamic model are compared with the predictions of Kaji and Okazaki[1] for the outgoing acoustic wave amplitudes due to rotor-stator interaction.

Acoustic Wave Generation by Rotor-Stator Interaction

Kaji and Okazaki[1] investigated the unsteady aerodynamic interaction of two rigid blade rows in relative motion to predict rotor-stator interaction noise. The mean flow was a uniform, compressible stream past two, two-dimensional cascades of flat plates aligned with the flow. For an assumed wake profile, they obtained a simultaneous solution to the unsteady lift distributions on both of the blade rows and determined the resulting outgoing acoustic waves.

The stagger angles of the blade rows are $\gamma_1 = -\gamma_2 = 30$ deg, giving identical relative Mach numbers for the two rows. The solidity of each row is 1, and the reduced frequency is π. Amplitudes of the first harmonic downstream acoustic waves are shown as a function of relative Mach number and the axial gap between the blade rows in Fig. 2. Predictions of the present method are in good agreement with those of Kaji and Okazaki.

Flutter

To investigate the effects of unsteady aerodynamic blade row interaction on flutter, two configurations of three blade rows were analyzed. The first configuration consists of a staggered rotor placed between unstaggered stators, whereas the second has an unstaggered stator between staggered rotors. To help isolate various effects, the stability of the middle blade row will be determined for three different cases:

1) The middle row is treated as if it is an isolated blade row, so there is no unsteady aerodynamic coupling between the blade rows (the "NC" solution).

2) Unsteady aerodynamic coupling occurs between the middle row and its neighbors, but the neighboring blade rows are rigid (the "AC" solution).

3) Unsteady aerodynamic coupling occurs and the secondary blade rows are now flexible, hence, the blade rows are dynamically coupled (the "DC" solution).

Variation of the blade row spacing as a technique for enhancing blade row stability will be investigated.

System parameters for configuration I are shown in Table 1. The axial Mach number relative to the stators is 0.4, and

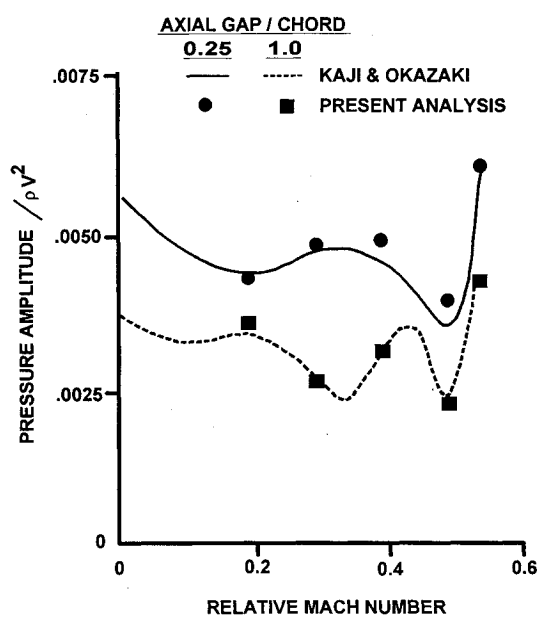

Fig. 2 Rotor-stator interaction noise: amplitude of downstream-running acoustic wave.

Table 1 Blade row configuration I

	Stator 1	Rotor	Stator 2
Blade row index, l	1	2	3
Chord, c	1	1	1
Solidity, c/s	1.5	1.4	1.5
Stagger angle, deg	0	60	0
Relative Mach number, M	0.4	0.8	0.4
Blade Mach number, U/a	0	−0.693	0
Elastic axis/chord	0.4	0.4	0.4
Radius of gyration	0.4	0.4	0.4
Mass ratio	200	200	200
Natural frequency, $\omega_{\alpha}/\omega_{\alpha\,\mathrm{Rotor}}$	1	1	1
Damping coefficient	0.5%	0.5%	0.5%

the rotor relative Mach number is 0.8. For the rotor geometry, mean-flow conditions and reduced frequency $\mathrm{Re}(\bar{\omega}_2) = 1$, acoustic resonances occur at $\beta_2 = -20.3$ deg, and $\beta_2 = 146.4$ deg. The radii of gyration and mass ratios are similar to those used by Chiang,[13] and are believed to be reasonable values for titanium compressor blades. For the initial calculations, the leading-edge loci of the blade rows are at axial locations −1.0, 0.1, and 1.5 chord, and so there is a 0.1-chord axial gap between the rotor and the upstream stator, and a 0.9-chord axial gap between the rotor and the downstream stator.

To obtain an equation of motion for the isolated rotor, the oscillations of the blade rows are decoupled by modifying the coefficient matrix A. In Eq. (8a), letting $C_{jl} = 0$ for all $l \neq j$, then substituting this A matrix into Eq. (9) results in

$$(S_2 + C_{22})\alpha_2 = 0 \tag{23}$$

for row 2. Thus, the oscillations of the blade rows are decoupled, but Eq. (23) still retains the effects of unsteady aerodynamic interaction between the blade rows through the coefficient C_{22}. Replacing C_{22} by the isolated blade row motion-induced moment $\hat{C}_2$ results in an equation for the isolated rotor:

$$(S_2 + \hat{C}_2)\alpha_2 = 0 \tag{24}$$

γ_2 is determined by solution of $S_2 + \hat{C}_2 = 0$, then the oscillation frequency is found from $i\omega_2/\omega_{\alpha 2} = i/\sqrt{\gamma_2}$. Similarly, the aerodynamic coupling solutions are obtained from Eq. (23) by solving $S_2 + C_{22} = 0$.

Isolated blade row (NC) solutions and aerodynamic coupling (AC) solutions for configuration I are shown in Fig. 3 for 15-deg increments in β_2; the corresponding values of β_2 are given adjacent to the points. The NC solutions indicate that the rotor is stable for all β_2 [$\mathrm{Re}(i\omega_2/\omega_{\alpha 2}) < 0$]. For subresonant values of β_2, $\beta_2 < -20.3$ deg, or $\beta_2 > 146.4$ deg, the AC solutions are identical to the NC solutions because decaying waves are neglected in the analysis. For super-resonant values of β_2, the AC solutions differ from the NC solutions, and some of the roots indicate flutter—the points 75 deg $\leq \beta_2 \leq$ 120 deg have all shifted far enough to the right that $\mathrm{Re}(i\omega_2/\omega_{\alpha 2}) > 0$.

Dynamic coupling solutions for configuration I are shown in Fig. 4. About 5 min of computing time on an 80486-based personal computer was required to obtain these solutions. Now that all of the blade rows are allowed to oscillate, there are three solutions at each super-resonant interblade phase angle. Where two solutions are difficult to distinguish from one another, (2) is placed next to the value of β_2. Two distinct groups of roots are shown in the figure—one group, with $\mathrm{Im}(i\omega_2/\omega_{\alpha 2}) \approx 1$, stretches horizontally across the plot, while the second group stretches vertically just to the stable side of the neutral stability line. The first group is replotted in Fig. 5 along with the AC solution first shown in Fig. 3. These two solutions are effectively identical, implying that the dynamics of the stator blades have a negligible effect on the rotor sta-

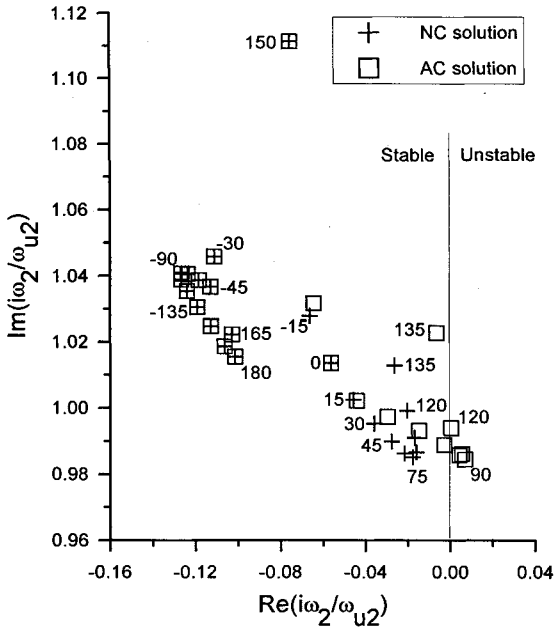

Fig. 3 Configuration I rotor stability: comparison of AC and NC solutions.

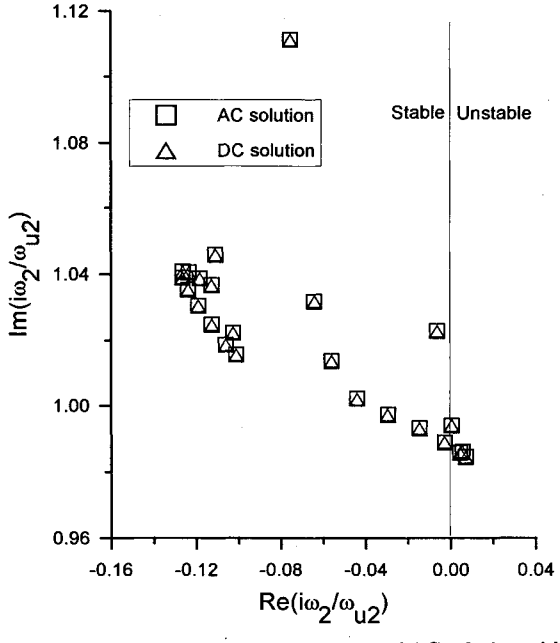

Fig. 5 Configuration I stability: comparison of AC solution with DC solution.

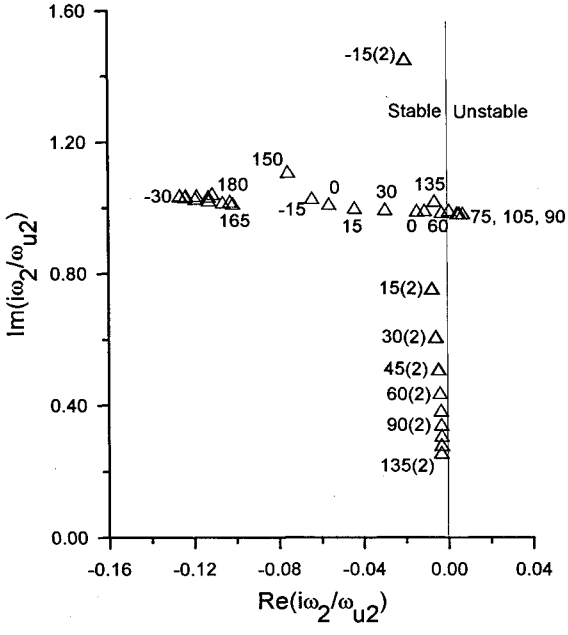

Fig. 4 Configuration I stability: DC solution.

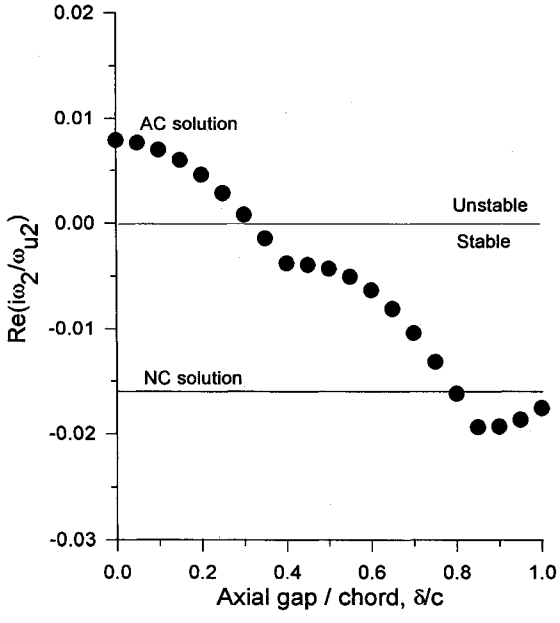

Fig. 6 Effect of axial gap on least stable solution, configuration I.

bility. Upon inspection of the coefficient matrix A for this configuration, it was found that the off-diagonal terms were small relative to the diagonal terms, thus, the oscillations of the blade rows were effectively decoupled due to weak unsteady aerodynamic interaction. Due to the decoupling, the remaining solutions—the vertical group of roots in Fig. 4—are interpreted as AC solutions for the stability of the two stators. The solutions for the stators are nearly identical despite their differing locations in the configuration, which indicates that unsteady aerodynamic coupling effects on them are also negligible. The frequencies of these solutions vary with interblade phase angle because they are presented in terms of the rotor frequency—the stators are oscillating near their natural frequencies, but due to the motion of the rotor, the frequency in the rotor frame varies with the interblade phase angle or tangential wave number.

Due to changes in wave interference patterns, the rotor stability will vary with spacing between it and the stators. Let δ be the distance between the rotor leading edge and the upstream stator trailing edge. Results for the present configuration are shown in Fig. 6; the positions of the stators are fixed while the rotor position between them is varied between $\delta/c = 0$ (rotor leading edge coincident with upstream stator trailing edge), and $\delta/c = 1$ (rotor trailing edge coincident with downstream stator leading edge). Relative to the isolated-rotor solution, the unsteady aerodynamic coupling effects are generally destabilizing, but for $\delta/c > 0.8$, a stabilizing effect occurs. The rotor is unstable for $\delta/c < 0.31$. These results suggest that blade row stability may be enhanced by variation of the blade row spacing. However, one should keep in mind that this solution was restricted to propagating waves and, as the blade row spacing decreases, the effects of decaying waves increase.

The stability of a second configuration was also analyzed: configuration II (Table 2) consists of an unstaggered stator between two identical rotor blade rows. The blade row spac-

Table 2 Blade row configuration II

	Rotor 1	Stator	Rotor 2
Blade row index, k	1	2	3
Chord, c	1	1	1
Solidity, c/s	1.5	1.3	1.5
Stagger angle, deg	60	0	60
Relative Mach number, M	0.8	0.4	0.8
Blade Mach number, U/a	−0.693	0	−0.693
Elastic axis/chord	0.5	0.5	0.5
Radius of gyration	0.4	0.4	0.4
Mass ratio	200	200	200
Natural frequency, $\omega_u/\omega_{u\,\mathrm{Rotor}}$	1	1	1
Damping coefficient	0.5%	0.5%	0.5%

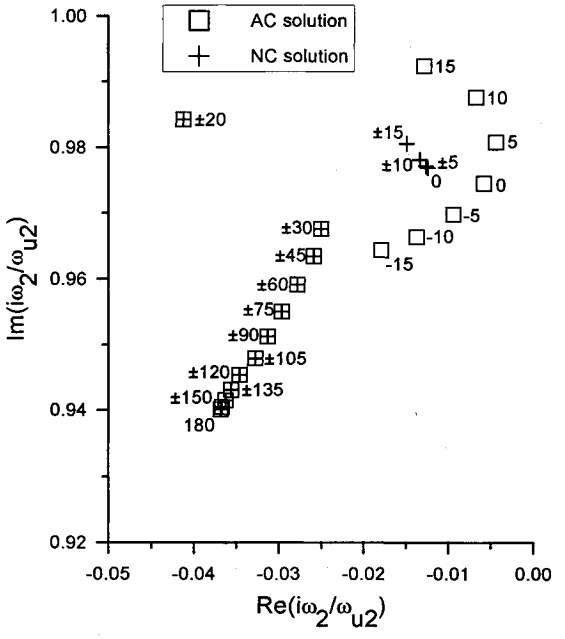

Fig. 7 Configuration II stator stability: AC vs NC solution.

ing was chosen so that a one-half chord axial gap separates the stator from each of the neighboring rotors. For the stator geometry, mean-flow conditions, and reduced frequency $\mathrm{Re}(\bar{\omega}_2) = 1$, the resonant interblade phase angles are ± 19.2 deg. Figure 7 shows the NC and AC solutions. The stator is stable in both cases, although aerodynamic interaction makes it less stable for some β_2. However, if the rotors are allowed to vibrate (Fig. 8), there are dramatic changes in the solution—there are two unstable values of β_2, 15 and 10 deg, and a number of other roots that are quite different from those for the AC solution. The dynamics of the neighboring blade rows, which were negligible for configuration I, play a crucial role in the stability of configuration II.

Forced Response

To investigate the effects of unsteady aerodynamic blade row interaction on forced response, calculations were made for the first harmonic response of the stator in configuration II due to the wakes of the upstream blade row. The stator reduced frequency is $\bar{\omega}_2 = 16.32$. In contrast to the stability solution procedure, where ratio of the oscillation frequency to the undamped natural frequency was the solution, the oscillation frequency is now fixed and the undamped natural frequency will be varied in order to see how the response varies in the vicinity of resonance.

The forced response of the configuration II stator is shown in Fig. 9 as a function of ω_2/ω_{u2}. The response parameter is the ratio of the oscillation amplitude with unsteady aerodynamic coupling effects to the oscillation amplitude for the isolated stator. At resonance, the AC response is nearly 45% greater than the NC response. Away from resonance, the AC response is still about 20% greater than the NC response. For this configuration, the DC response was essentially identical to the AC response—the oscillations of the rotors did not affect the stator.

A brief parametric study of the effects of blade row spacing and rotor solidity on the stator forced response was made. Configuration II was used for this study along with two configurations identical to it, except for changes in the rotor solidities. The gap between the stator and the upstream rotor was varied between 0–1 chord; with a gap of one chord, the stator trailing edge was coincident with the leading edge of the downstream rotor. As shown in Fig. 10, the response of the stator can vary greatly with these parameters. With the higher solidity rotors $[(c/s)_1 = (c/s)_3 = 1.55)]$, the stator response amplitude varies between exceeding the isolated stator response by nearly 60% to being 15% less than it. In contrast, with the lower solidity rotors $[(c/s)_1 = (c/s)_3 = 1.45)]$, the

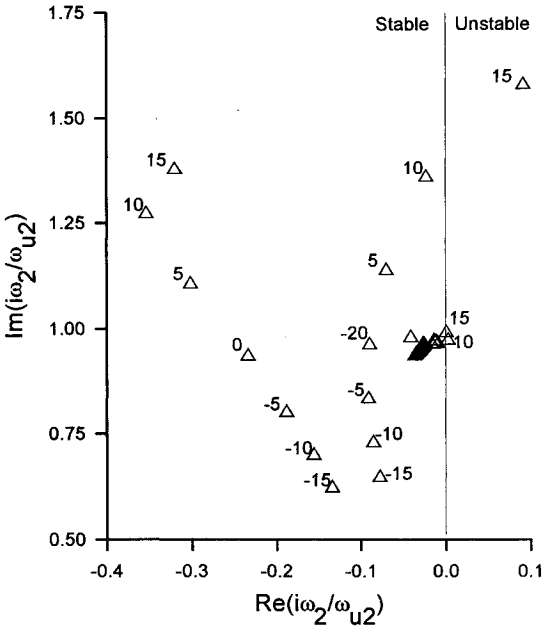

Fig. 8 Configuration II stability: DC solution.

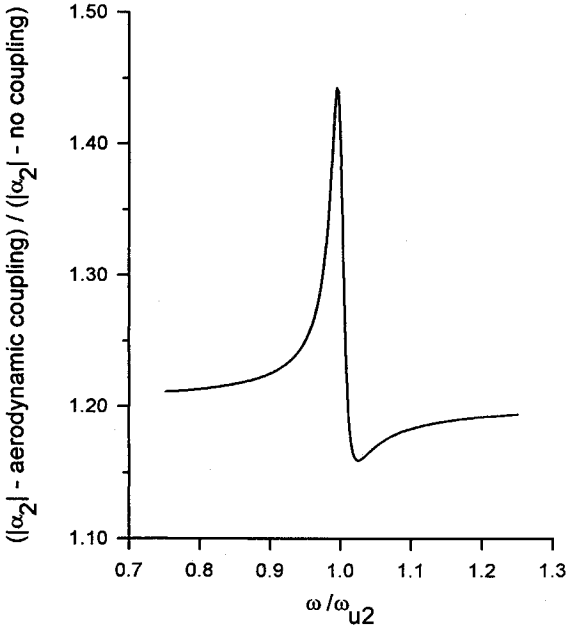

Fig. 9 Forced response of configuration II stator vs frequency.

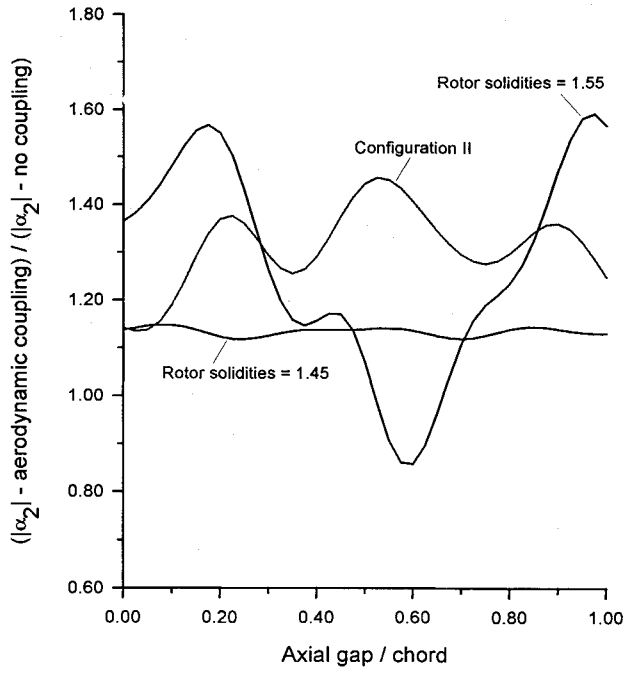

Fig. 10 Effect of blade row spacing and rotor solidities on peak stator forced response.

stator response varies little with axial gap, staying about 13% greater response than the isolated stator.

Summary and Conclusions

The effects of blade row unsteady aerodynamic interaction on flutter and forced response have been investigated. A model for interaction between any number of blade rows was developed that relies upon unsteady aerodynamic coefficients obtained from isolated blade row analyses. Using influence coefficients that express the unsteady forces on one blade row due to the motion of another, an aeroelastic model was obtained that accounts for coupling of the vibratory responses of multiple blade rows, or dynamic coupling between the blade rows. A special case of this model is obtained when neighbors of the blade row under consideration are assumed to be rigid, but the unsteady aerodynamic coupling between these neighbors is retained.

This analysis technique was applied to two model configurations, each consisting of three blade rows. Stability solutions were found for each configuration. For the first configuration, aerodynamic coupling had a destabilizing influence relative to the isolated blade row solution. The additional effect of dynamic coupling was negligible relative to the aerodynamic coupling effect. In contrast, the dynamic coupling analysis indicated flutter for the second configuration while the unsteady aerodynamic coupling solution and the isolated blade row solution both predicted stability.

The forced response analysis was applied to one baseline configuration. Significant increases in the response amplitude were found to occur due to unsteady aerodynamic coupling. A parametric study showed that blade row spacing and solidity can have significant effects on the response amplitude.

Acknowledgments

This research was supported by the Turbomachinery Technology Branch, Propulsion Systems Division of the NASA Lewis Research Center. D. Hoyniak, D. Huff, and L. Bober, all of NASA, and F. McCaughan of Case Western Reserve University, Cleveland, Ohio, provided helpful comments on the content of this article.

References

[1]Kaji, S., and Okazaki, K., "Generation of Sound by Rotor-Stator Interaction," *Journal of Sound and Vibration*, Vol. 13, No. 3, 1970, pp. 281–307.

[2]Hanson, D. B., "Unsteady Coupled Cascade Theory Applied to the Rotor/Stator Interaction Noise Problem," DGLR/AIAA Paper 92-02-084, May 1992.

[3]Smith, S. N., "Discrete Frequency Sound Generation in Axial Flow Turbomachines," Aeronautical Research Council Reports and Memoranda 3709, Her Majesty's Stationery Office, London, March 1972.

[4]Chen, S. H., and Williams, M. H., "Panel Method for Counter-Rotating Propfans," *Journal of Propulsion and Power*, Vol. 7, No. 4, 1991, pp. 593–601.

[5]Williams, M. H., Cho, J., and Dalton, W. N., "Unsteady Aerodynamic Analysis of Ducted Fans," *Journal of Propulsion and Power*, Vol. 7, No. 5, 1991, pp. 800–804.

[6]Rai, M. M., "Navier-Stokes Simulations of Rotor/Stator Interaction Using Patched and Overlaid Grids," *Journal of Propulsion and Power*, Vol. 3, No. 5, 1987, pp. 387–396.

[7]Jorgensen, P. C. E., and Chima, R. V., "Explicit Runge-Kutta Method for Unsteady Rotor-Stator Interaction," *AIAA Journal*, Vol. 27, No. 6, 1989, pp. 743–749.

[8]Giles, M. B., "Stator/Rotor Interaction in a Transonic Turbine," *Journal of Propulsion and Power*, Vol. 6, No. 5, 1990, pp. 621–627.

[9]Whitehead, D. S., "Classical Two-Dimensional Methods," *AGARD Manual on Aeroelasticity in Axial-Flow Turbomachines, Volume 1, Unsteady Turbomachinery Aerodynamics*, edited by M. F. Platzer and F. O. Carta, AGARD-AG-298, March 1987.

[10]Verdon, J. M., "Linearized Unsteady Aerodynamics for Turbomachinery Aeroelastic Applications," AIAA Paper 90-2355, July 1990.

[11]Hall, K. C., and Clark, W. S., "Prediction of Unsteady Aerodynamic Loads in Cascades Using the Linearized Euler Equations," AIAA Paper 91-3378, June 1991.

[12]Fang, J., and Atassi, H. M., "Compressible Flows with Vortical Disturbances Around a Cascade of Loaded Airfoils," *Unsteady Aerodynamics, Aeroacoustics, and Aeroelasticity of Turbomachines and Propellers*, edited by H. M. Atassi, Springer–Verlag, New York, 1993, pp. 149–176.

[13]Chiang, H.-W. D., "Aerodynamic Detuning of a Loaded Cascade in an Incompressible Flow by a Locally Analytical Method," Ph.D. Dissertation, Purdue Univ. School of Mechanical Engineering, West Lafayette, IN, 1988.

[14]Buffum, D. H., "Blade Row Interaction Effects on Flutter and Forced Response," AIAA Paper 93-2984, June 1993.